Expanded austenite; from fundamental understanding to predicting composition- and stress-depth profiles

Somers, Marcel A. J.; Christiansen, Thomas L.; Winther, Grethe

Publication date:
2018

Document Version
Peer reviewed version

Expanded austenite; from fundamental understanding to predicting composition- and stress-depth profiles

Marcel A. J. Somers, Thomas L. Christiansen, Grethe Winther

Department of Mechanical Engineering, Technical University of Denmark, Produktionstorvet b. 425, 2800 Kgs. Lyngby, Denmark, somers@mek.dtu.dk

Abstract

The case developing during low temperature surface hardening of austenitic stainless steel by nitriding, carburising or nitrocarburising consists of a supersaturated interstitial solid solution of nitrogen and/or carbon in austenite. The favorable properties of this so-called expanded austenite depend on the profiles of interstitial concentration and associated composition-induced residual stress over the case. In the present contribution an overview of the current state of understanding of the evolution of the microstructure, composition and residual stress during low temperature surface hardening of stainless steels is presented. The manuscript showcases the joint achievements of many co-workers in the last 18 years. The overview concerns theoretical, experimental and modelling aspects of expanded austenite, both as a homogeneous phase and as a case on stainless steel.

Keywords

Expanded austenite, stainless steel, residual stress, numerical modelling

1 Introduction

Since the mid-eighties of the previous century surface hardening of austenitic stainless steel by the dissolution of nitrogen and/or carbon atoms has developed into a commercially successful remedy against galling and wear, and has further improved the pitting and crevice corrosion. For a description of the historical development, the process variants, including plasma, gaseous and liquid baths, as well as the obtainable properties and performance improvement, the reader is referred to recent comprehensive reviews of the topic [Christiansen, Somers 2009, Dong 2010, Somers, Christiansen 2014, 2015, Fernandes, Christiansen, Somers 2015]. The microstructure developing during low temperature surface hardening of stainless steel consists of a zone of a supersaturated solid solution of interstitial atoms (N and/or C) in austenite, so-called expanded austenite (or S-phase). Expanded austenite refers to an expansion of the crystal lattice as a consequence of the (colossal) interstitial content in supersaturated solid solution. Since expanded austenite is not a separate phase, the terminology S-phase is considered inappropriate and therefore not practiced here. As a consequence of the enormous content of interstitials in expanded austenite, huge compressive residual stresses are induced. The present contribution reviews the current understanding of the developing case of expanded austenite during gaseous nitriding in terms of composition and residual stress in order to arrive at a numerical model to predict the composition and stress. Similar considerations may apply for carburising of stainless steels, albeit to a lesser extent, because the carbon solubility in supersaturated solution is appreciable lower than the nitrogen solubility.

2 Nitriding of stainless steel without nitride formation

Thermodynamically, the interstitial solubility of the nitrogen in austenitic stainless steel is very low and will readily lead to the development of nitrides. The nitride forming constituent of concern is chromium, which is the main alloying element in stainless steels to provide the protection against corrosion. Removing chromium from solid solution by nitride formation jeopardizes the inherent corrosion protection as chromium is no longer abundantly present to develop a passivating oxide layer at the surface. Only for relatively high temperatures, say above 1250 K is nitrogen dissolved in austenite to a certain extent, without nitride formation (cf. Figure 1). Industrially, such treatments are known as high temperature solution nitriding (HTSN) [Berns et al. 2000], and the nitrogen content in solid solution can be readily adjusted by choosing the right combination of temperature and N_2 pressure in the gas (Figure 1a). HTSN entails fast gas quenching in order to avoid nitride/carbide formation at intermediate temperatures. Kinetically, the development of chromium nitrides can be delayed by dissolving nitrogen at a relatively low temperature. This is illustrated in Figure 1 in a schematic TTT diagram and referred to as "low temperature surface hardening". At relatively low temperatures the interstitial nitrogen atoms are mobile as they diffuse over the octahedral interstices of the austenite lattice, while the substitutionally dissolved chromium atoms diffuse very slowly. Consequently, in the competition between interstitial diffusion and nitride formation, a certain depth can be reached by the interstitial atoms before the first nucleation of chromium-based nitrides.

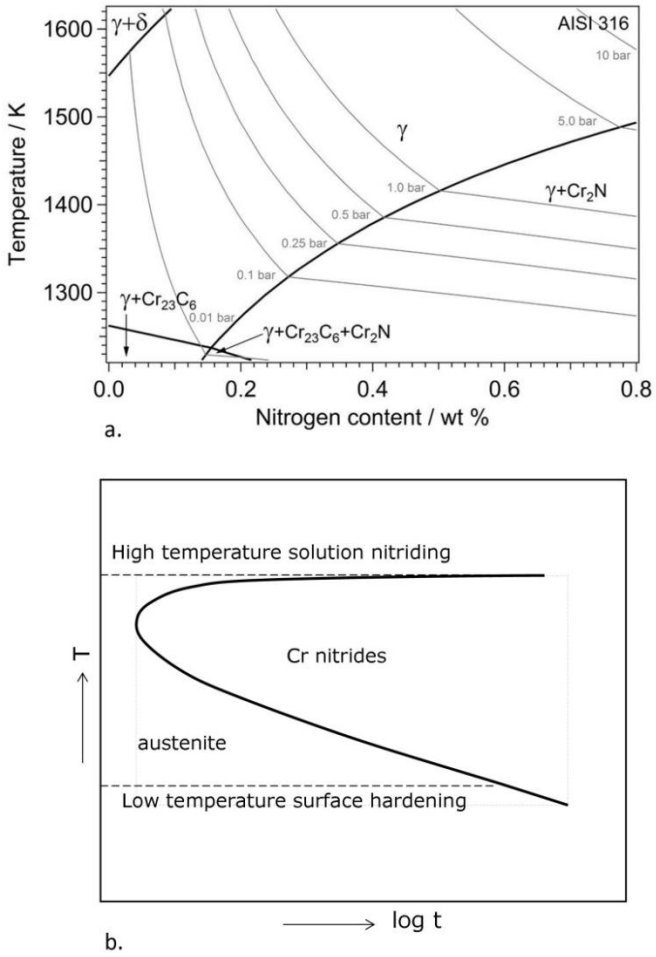

Figure 1: (a) Isopleth for AISI 316 with various nitrogen contents calculated with ThermoCalc using database TCFE7. The grey lines are isobars for the N_2 pressure [Bottoli et al. 2016]. (b) Schematic TTT diagram for nitrogen/carbon containing austenite, showing the time available before chromium nitrides/ carbides develop. High-temperature solution nitriding can be performed for temperatures where austenite is stable and the equilibrium content follows from the combination of temperature and isobar in (a).

In a solid solution in fcc, Cr tries to obtain as many nitrogen atoms in the neighbouring octahedral interstices as possible. Experimentally Cr:N ratios in excess of 1:3 have been observed [Christiansen, Somers 2006], where on average each Cr atom has 5 N neighbours [Oddershede et al. 2010]. Also, since there is a strong affinity between chromium and nitrogen atoms, a high meta-stable solubility of nitrogen can be reached, which by far exceeds the nitrogen content that can be bound as CrN and dissolved in the austenite matrix. This implies that a (strongly) supersaturated solid solution of interstitials is obtained.

3 Properties of homogeneous expanded austenite

The effect of the dissolution of interstitial atoms in austenite at low temperatures on the lattice parameter of austenite has been experimentally determined for stress-free homogeneous powders and foils [Christiansen, Somers 2006, Hummelshøj, Christiansen, Somers 2010, Brink et al. 2016] and shows an expansion of up to 11 % in the lattice parameter. See in this respect Figure 2a where the stress-free lattice parameter is given as a function of the occupancy of octahedral interstices, y_N (or y_C), which equals the number of interstitials per metal atom for fcc. The discontinuity at $y_N = 0.17$ is a consequence of a magnetic transition in austenite [Brink et al. 2016]. For intermediate nitrogen contents expanded austenite has a Curie temperature at about 550 K, while for low and very high nitrogen contents the Curie temperature is below room temperature (Figure 2b). This dependence of the magnetic properties on the nitrogen content is also reflected in the thermal expansion coefficient, which shows a discontinuous change at the Curie temperature (Figure 2c) and vary low values for ferromagnetic expanded austenite (Figure 2d).

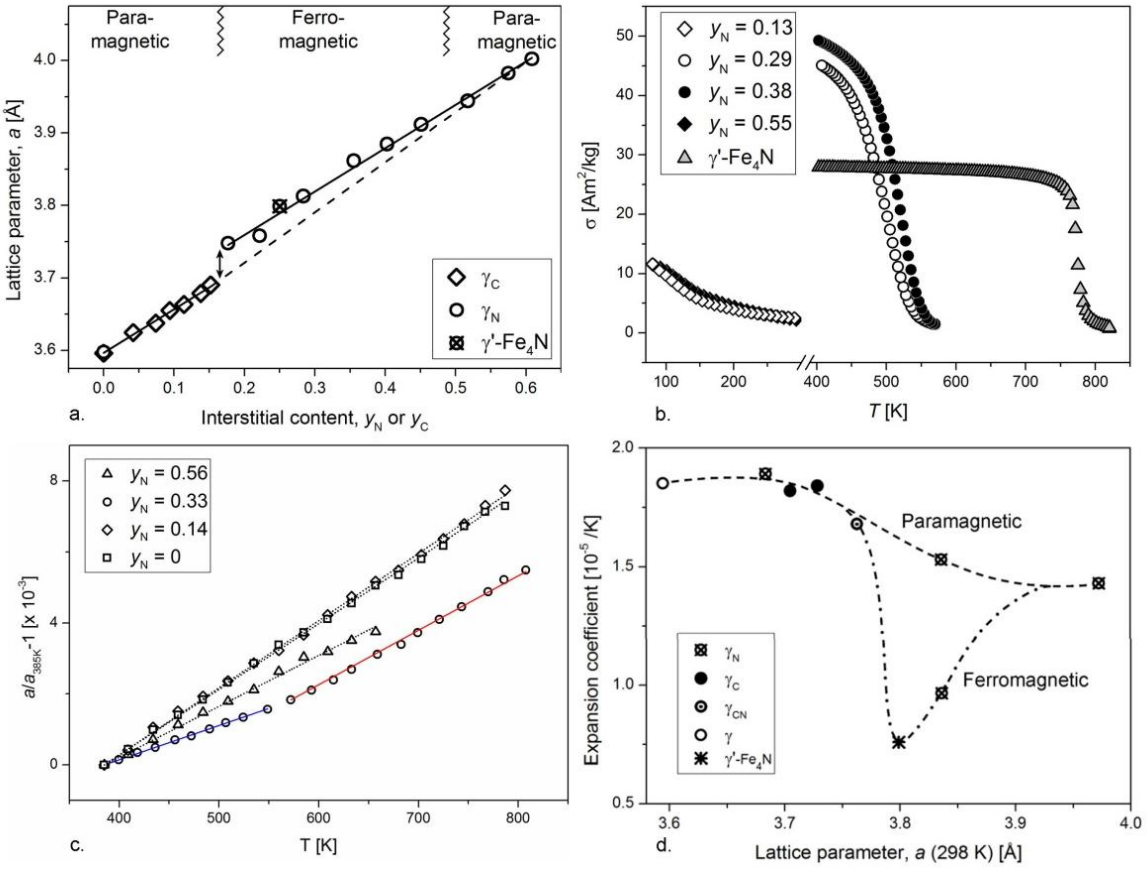

Figure 2: Expansion of austenite lattice parameter (a) as a consequence of interstitially dissolved nitrogen and carbon (a); the saturation magnetization (σ) and the Curie temperature depends on the dissolved nitrogen content (b); linear thermal expansion is also dependent on the interstitial content and shows a discontinuous change at the Curie temperature (c, d) [Brink et al. 2016]

Analogous to ferritic nitriding, the equilibrium solubility of nitrogen in expanded austenite can be adjusted by the nitriding potential, which is linearly proportional to the thermodynamically defined nitrogen activity, a_N (Fig.3a). The diffusivity of nitrogen in strain-free expanded austenite of uniform composition was determined as a function of the dissolved nitrogen content and depends strongly on the interstitial content (Figure 3b) as a consequence of antagonistic effects of lattice expansion and site occupancy on the interstitial lattice [Christiansen, Somers 2008]. The thermal stability of expanded austenite is limited as there is a large driving force for the development of CrN. In-situ synchrotron X-ray diffraction studies have demonstrated that for high nitrogen contents the thermal stability is reduced and that an intermediate phase develops with a lattice parameter commensurate with γ'-Fe_4N, and indicated as γ_T in Figure 3c, which decomposes into ferrite and CrN (Figure 3c) [Brink et al. 2014].

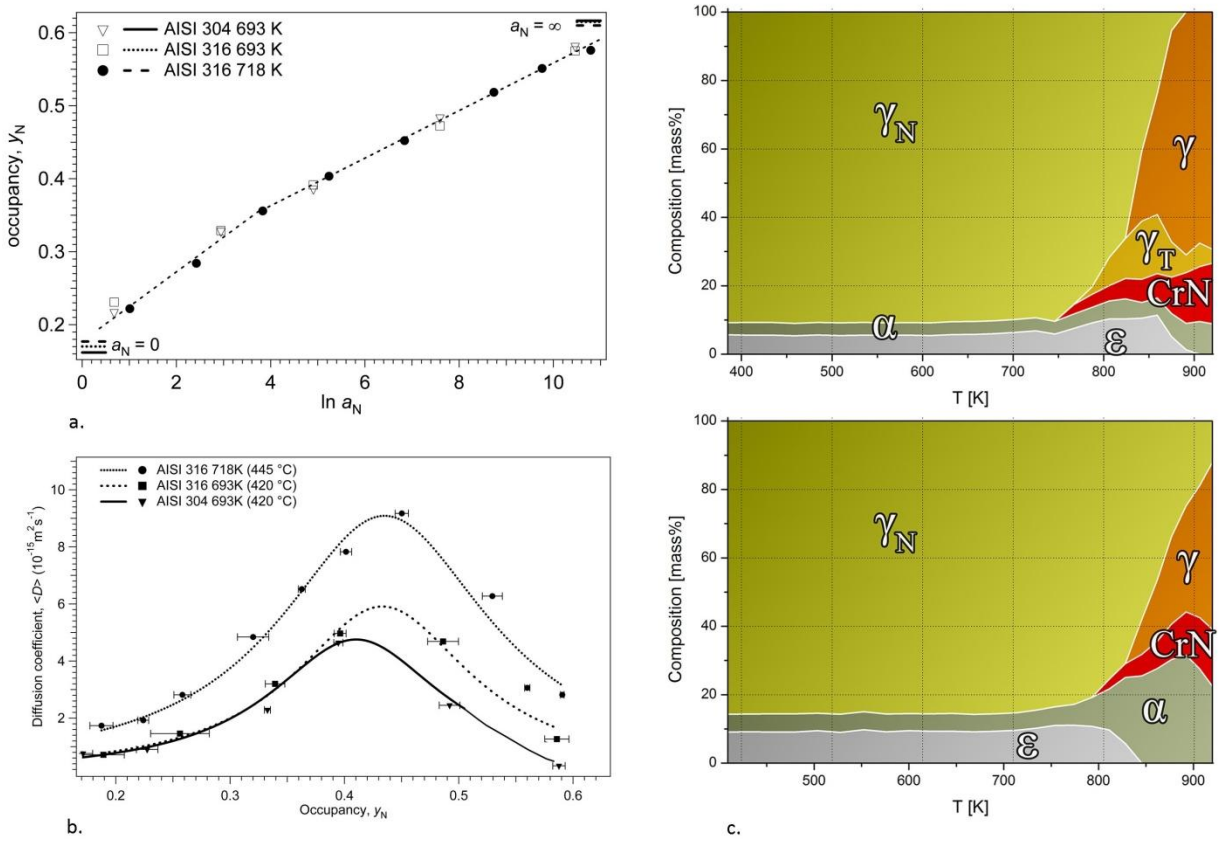

Figure 3: The equilibrium nitrogen content in expanded austenite can be adjusted by the nitrogen activity as imposed by the nitriding potential of a NH_3/H_2 gas mixture (a) [Christiansen, Somers 2006]; the nitrogen diffusivity depends strongly on the nitrogen content [Christiansen, Somers 2008]; decomposition of expanded austenite occurs beyond 750 K during linear heating and develops CrN and α in addition of γ (c. top $y_N = 0.56$, bottom $y_N = 0.14$) [Brink et al. 2014].

4 Residual stress in expanded austenite on surface hardened stainless steel

In practice expanded austenite is not used as a thin foil of uniform composition, but as a case reaching to a certain depth into austenitic stainless steel with a concentration-depth profile. Figure 4a shows a nitrogen concentration depth-profile, while the shift of 111 and 200 line profiles to lower Bragg angles is shown for different depths in Figure 4b [Fernandes et al. 2015B]. As a consequence of the lattice expansion associated with nitrogen dissolution the concentration profile leads to a profile in lattice expansion (Figure 4c), which is accommodated by residual compressive stress (Figure 4d). The experimental determination of residual stresses in expanded austenite with X-ray diffraction techniques is challenged by the presence of (steep) gradients which affect the quantitative values and necessitates special measurement procedures

or correction procedures to determine the actual values [Fernandes et al. 2015B, Christiansen, Somers 2006B]. The residual stress values shown in Figure 4d were determined with grazing-incidence X-ray diffraction stress determination; for further details see [Fernandes et al. 2015B]. The depth profile was determined from repeated layer removal by careful polishing and etching. The maximum stresses that were determined by this stress determination method are approximately 5 GPa in compression.

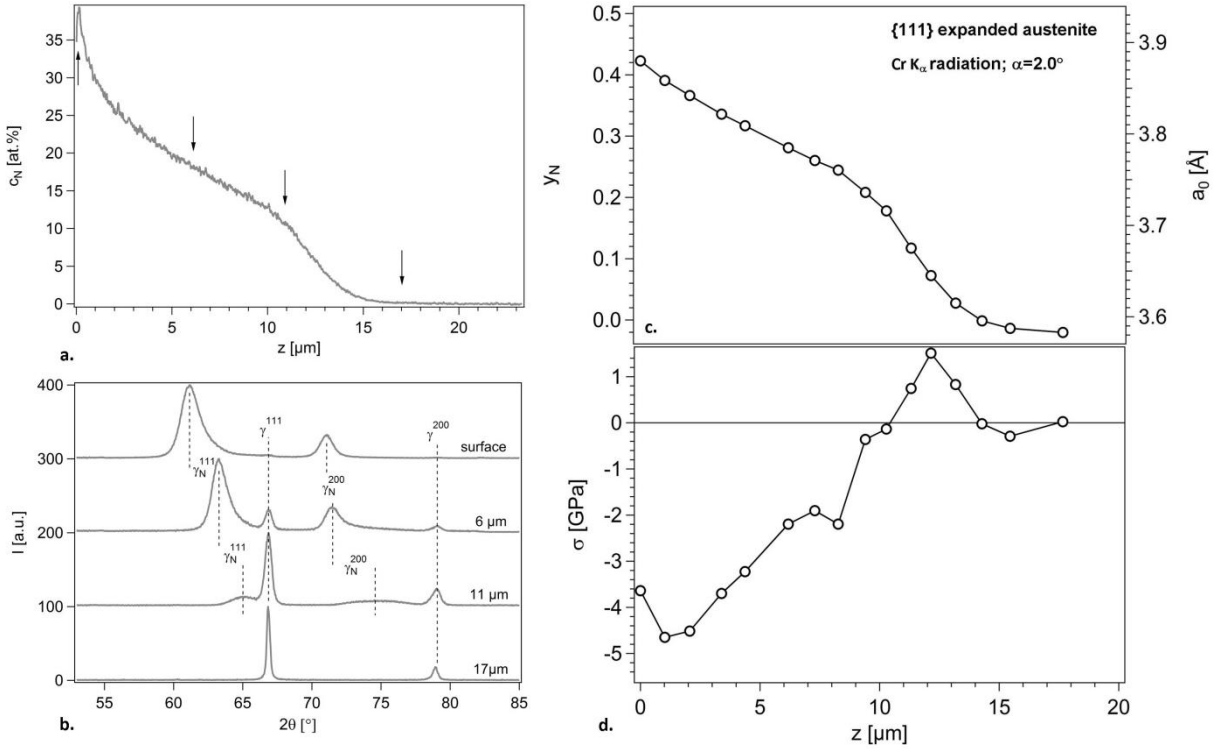

Figure 4: (a) Nitrogen profile obtained with GD-OES and (b) X-ray diffractograms of the AISI 316L steel gas nitrided at 703 K for 20 h obtained by symmetric X-ray diffraction. From top to bottom: as-nitrided surface and after removing 6 µm, 11 µm and 17 µm. The latter corresponds to un-treated bulk austenite. The arrows in the GD-OES profile show the (approximate) positions of the surface positions for the diffractograms in b;(c) profile of the strain-free lattice parameter (a_0) determined from grazing incidence stress measurements and the corresponding nitrogen content y_N; (d) depth distribution of elastic residual stress [Fernandes et al. 2015B]. The sample was nitrided at 703 K in NH_3 for 20 h.

The colossal dissolution of interstitials into austenite leads to most effective solid solution strengthening, implying an increase of the yield stress and the hardness. It is this increase in hardness, routinely reaching 12 GPa, which is the objective of the treatment, to enhance the wear (and galling) resistance without impairing the corrosion resistance (hence the prevention of nitrides). It has been demonstrated that full elastic accommodation of the lattice expansion leads to unrealistically high compressive stresses of about 30 GPa in compression, which by far outweigh the yield strength of the solution strengthened stainless steel of about 4 GPa [Jespersen, Hattel, Somers 2016]. Consequently, also plastic accommodation of the lattice expansion occurs, which is manifested as lattice rotation, surface roughening and eventually grain push out and brittle fracture [Christiansen, Somers 2006, Templier et al. 2010]. An example of lattice rotations of gaseously nitrided austenitic stainless steel measured over the expanded austenite zone is given for three tracks in Figure 5 [Somers et al. 2018]. The corresponding rotation is presented in the inverse pole figures (bottom row) along and in the directions of the lines in the top-row image quality maps. Shear bands inclined with the surface are observed in expanded austenite for grains 2 (and the right-hand neighbour of grain 3).

In addition to the composition profile which leads to chemically induced strains (and associated stresses) at the nitriding temperature, the change in thermal expansion with interstitial content

(Figure 2) leads to a gradient in thermal shrink during cooling from the treatment temperature. This leaves a complicated state of stress in the expanded austenite zone.

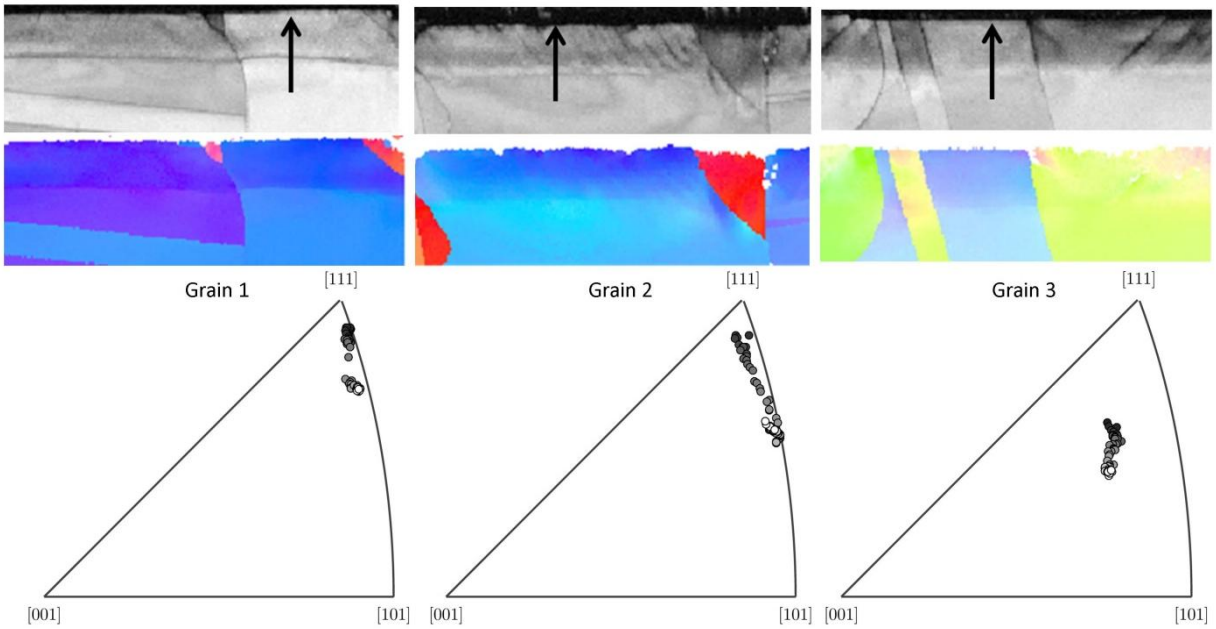

Figure 5: EBSD results of AISI 316 nitrided for 713 K for 8 h in pure NH_3. Top row shows image quality maps (IQM); second row shows orientation image maps (OIM). For the locations of the arrows the rotation of the lattice is given in the inverse pole figures (IPF), starting in the unaffected AISI 316 for the white dots and moving towards increasingly darker dots [Somers et al. 2018].

For low interstitial contents elastic strains are observed, while for higher interstitial contents plastic strains are superimposed onto the elastic strains. In addition to the volume expansion by interstitial dissolution at the treatment temperature, the introduction of concentration dependent thermal strains can be expected upon cooling to room temperature. Depending on the actual yield strength, which also depends on temperature, these thermal strains are elastically or plastically accommodated.

5 Modelling of composition and residual stress

Various attempts to predict the composition profile over the expanded austenite layer have been published. Two essentially different approaches have been put forward to explain the shape of the nitrogen (or carbon) concentration profile: i) a composition dependent diffusivity of the interstitials [Christiansen, Dahl, Somers 2008] or ii) a gradient in the trapping-detrapping of interstitials by trap sites (Cr atoms) in combination with a constant, hkl-dependent diffusivity [Martinavičius, Abrasonis, Möller 2011]. An hkl-dependent diffusivity is in contradiction with the isotropy of diffusion in cubic lattices. Recognizing the enormous compressive stress (gradient) the role of stress on the evolution of the composition profile in expanded austenite can be substantial [Somers, Christiansen 2005]. The role of the elastic residual stress and the cross-correlation between stress and composition by considering the effect of stress on the nitrogen solubility and on diffusion kinetics by stress-enhanced diffusion were considered [Christiansen, Somers 2010, Moskalioviene, Galdikas 2012, Jespersen, Hattel, Somers 2016]. Jespersen et al. [2016] included the occurrence of plasticity for residual stresses beyond the composition-dependent yield stress and demonstrated a satisfactory agreement between the level of elastic residual stress of –5 GPa at the surface, as shown in Figure 4. The explicit finite-difference model presented in [Jespersen, Hattel, Somers 2016] and modified to an implicit finite-difference model to allow inverse modelling [Kücükyildiz et al. 2017] consists of a thermal, a thermochemical part and a mechanical part. The yield stress of expanded austenite has so far not been determined experimentally and was estimated from the relation between hardness and

composition on the one side and an extrapolation of the relation between yield stress and hardness, on the other side [Jespersen, Hattel, Somers 2016], leading to a yield stress in plane stress of about –4 GPa.

For the mathematical expressions involved in the numerical model to calculate composition and stress profiles, the reader is referred to [Jespersen, Hattel, Somers 2016, Kücükyildiz et al. 2018]. To calculate the nitrogen concentration- and stress-depth profiles, the only input parameters are temperature, nitriding potential, nitriding time and yield stress. All other parameters were taken as those determined for homogenous stress-free thin foils (cf. Figure 2 for the lattice expansion leading to chemically-induced stress), the equilibrium concentration from Figure 2a and the concentration-dependent diffusivity of nitrogen in expanded austenite from Figure 2b. No fit parameters were used. More details are provided in a forthcoming publication [Kücükyildiz et al. 2018]. The purpose of the modelling attempts is to explore the various influences and in particular the role of plastic deformation. Figure 6a presents the concentration and elastic residual stress profiles calculated for nitriding AISI 316 at 440 °C for 4 h, 8 h and 16 h in pure ammonia. Clearly, the surface concentration of nitrogen in expanded austenite increases with treatment time and the concentration- and stress-profiles penetrate gradually into the austenite. The increase of the surface concentration with time is the outcome of a competition between the flux of nitrogen atoms arriving at the surface by ammonia dissociation and the flux of nitrogen atoms leaving the surface by inward diffusion. A comparison of the concentration- and stress-profiles to those in Figure 4a/c shows a qualitative agreement for the nitrogen concentration profile. The calculated stress-depth profile is characterised by a plateau stress value of –4.1 GPa, which was not found in the measured profile in Figure 4b. Nevertheless the magnitude of the maximum compressive stress is in good correspondence with the experimental values. The occurrence of a constant elastic stress is attributed to the assumption of constant yield stress of 4 GPa for nitrogen contents beyond $y_N \sim 0.1$. Figure 6b shows how the strains are accommodated by the expanded austenite as elastic strains ($\varepsilon_{11}^{el} = \varepsilon_{22}^{el}$) within the plane of the expanded austenite zone and plastic strain (ε_{33}^{pl}) in the direction perpendicular to the surface.

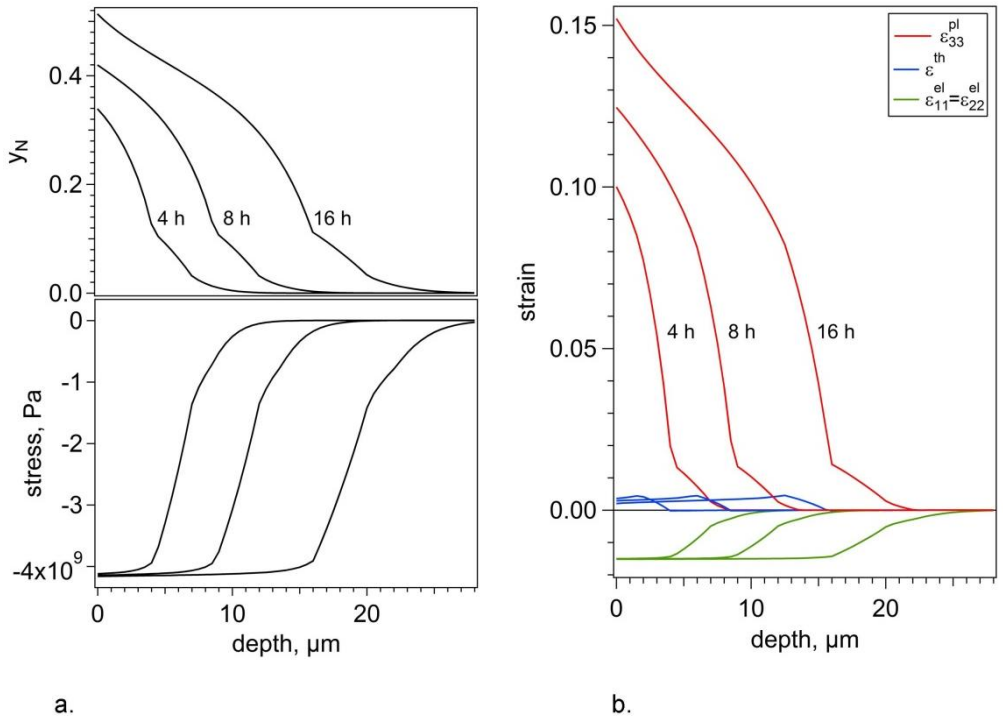

Figure 6: Calculated composition-depth and (elastic) residual stress-depth profiles for 4 h, 8 h and 16 h nitriding of AISI 316 at 713 K (a) and corresponding elastic strains within the plane of the expanded austenite zone ($\varepsilon_{11}^{el} = \varepsilon_{22}^{el}$), the plastic strain parallel to the surface normal (ε_{33}^{pl}) and the thermal strain ε^{th}

as a consequence of a variation in thermal expansion coefficient with interstitial content (cf. Figure 3) [Somers et al. 2018].

Evidently, substantial plastic strains are introduced by dissolving nitrogen. Comparing Figure. 6a and 6b leads to the conclusion that the continued uptake of nitrogen beyond $y_N \sim 0.1$ is fully accommodated plastically. Figure 6b also shows the additional thermal strains (ε^{th}) introduced on cooling from the treatment temperature to room temperature as a consequence of a variation of the linear expansion coefficient with the interstitial content (cf. Figure 2). The decrease in thermal expansion coefficient with nitrogen content in expanded austenite will lead to an additional compressive strain parallel to the surface particularly below the Curie temperature for the ferromagnetic expanded austenite. If the thermal strains are accommodated elastically, the thermal strain,ε^{th} , is added to $\varepsilon_{11}^{el} = \varepsilon_{22}^{el}$. If no additional elastic accommodation of the strain is possible during cooling after nitriding, the strain is accommodated plastically in the direction perpendicular to the surface. The blue lines in Figure 6b are given for the case that no additional elastic accommodation is possible.

The model applied to obtain the results in Figure 6 considers relevant parameters that determine the influence on the composition and stress profiles and provides consistent qualitative correspondence between experiment and prediction, including the degree of plastic deformation (see [Somers et al. 2018]). No exact correspondence is obtained, because not all parameters are quantitatively known. Obviously, the temperature dependence of elastic and plastic properties are currently insufficiently known and therefore not taken into account. Furthermore the current results were obtained under the assumption that expanded austenite behaves elastically and plastically isotropic. This is far from realistic, because austenite is strongly elastically anisotropic; the Young's modulus varies by a factor 3 between 100 and 111 measurement directions. Also, plastic anisotropy occurs, as slip can only occur along 111 planes. These topics are addressed in another presentation at this conference.

6 Conclusion

The present contribution shows the considerations necessary to arrive at a simulation of composition and residual stress profiles over the expanded austenite zone developing during gaseous nitriding of austenitic stainless steel under conditions of low temperature where no chromium nitrides develop during treatment time.

Essentially, thermodynamics and diffusion kinetics govern the evolution of the nitrogen concentration profile. Investigation of homogenous foils and powders of uniform composition provided the nitrogen solubility in dependence of the chemical potential of nitrogen as well as the composition dependence of the diffusion coefficient of nitrogen without the effect of mechanical stress. The thermal expansion coefficient of expanded austenite is composition dependent and is affected by the occurrence of ferromagnetism for an intermediate range of interstitial contents.

Elastic stress has an important influence on the nitrogen solubility and stress-induced diffusion and should be taken into account. Even though the dissolution of nitrogen leads to solid-solution strengthening, the enormous lattice expansion is largely accommodated plastically at the nitriding temperature. On cooling, the composition-dependent thermal expansion coefficient leads to additional residual stresses.

Acknowledgement

The research results presented in this contribution were obtained over many years of intensive research by many former and current co-workers. Through the years financial support has been obtained from various sources, which have been acknowledged in the original papers mentioned in the list of references.

References

Berns, H.; Juse, R.L.; Bouwman, J.W.; Edenhofer, B.: Solution nitriding of stainless steels-a new thermochemical heat treatment process, *Heat Treat. Met.*, Vol. 27, No. 2, 2000, pp.39-45.

Bottoli, F.; Winther, G.; Christiansen, T.L.; Dahl, K.V.; Somers, M.A.J.: Low-temperature nitriding of deformed austenitic stainless steels with various nitrogen contents obtained by prior high-temperature nitriding, *Metall. Mater. Trans.*, Vol. 47, No.8, 2016, pp. 4146-4159.

Brink, B.; Ståhl, K.; Christiansen, T.L.; Somers, M.A.J.: Thermal expansion and phase transformations of nitrogen-expanded austenite studied with in-situ synchrotron X-ray diffraction, *J. Appl. Cryst.* 47, 2015, pp. 819-826.

Brink, B.K.; Ståhl, K.; Christiansen, T.L.; Frandsen, C.; Hansen, M.F.; Somers, M.A.J.: Composition-dependent variation of magnetic properties and interstitial ordering in homogeneous expanded austenite, *Acta Mater.*, Vol. 106, 2016, pp. 32-39.

Christiansen, T.L.; Dahl, K.V.; Somers, M.A.J.: Nitrogen diffusion and nitrogen depth profiles in expanded austenite: experimental assessment, numerical simulation and role of stress, *Mater. Sci. Techn.*, Vol. 24, No. 2, 2008, pp. 159-167.

Christiansen, T.; Somers, M.A.J.: Controlled dissolution of colossal quantities of nitrogen in stainless steel, *Metall. Mater. Trans.*, Vol. 37A, No. 3, 2006, pp. 675-682.

Christiansen, T.; Somers, M.A.J.: Avoiding ghost stress on reconstruction of stress- and composition depth profiles from destructive X-ray diffraction depth profiling, *Mater. Sci. Eng. A*, Vol. 424, 2006B, pp. 181-189.

Christiansen, T.; Somers, M.A.J.: Determination of composition dependent diffusion coefficient of nitrogen in expanded austenite, *Int. J. Mater. Res.*, Vol. 99, No. 9, 2008, pp. 999-1005.

Christiansen, T.L.; Somers, M.A.J.: Low temperature gaseous surface hardening of stainless steel; the current status", *Int. J. Mater. Sci.*, Vol. 100, No. 10, 2009, pp. 1361-1377.

Christiansen, T.L.; Somers, M.A.J.: The influence of stress on diffusion - carbon diffusion data in austenite revisited, *Defect Diff. Forum*, Vols. 297-301, 2010, No.2, pp. 1408-1413.

Dong, H.: S-phase surface engineering of Fe-Cr, Co-Cr and Ni-Cr alloys, *Int. Mater. Rev.*, Vol. 55, No.2, 2010, pp. 55-98.

Fernandes, F.A.P.; Christiansen, T.L.; Somers, M.A.J.: Surface Hardening: Low Temperature *Encyclopedia of Iron, Steel, and Their Alloys*. In: Colas, R. and Totten, G.A., Taylor and Francis, New York, 2015, pp. 3502-3524.

Fernandes, F.A.P.; Christiansen, T.L.; Winther, G.; Somers, M.A.J.: On the determination of stress profiles in expanded austenite by grazing incidence X-ray diffraction and successive layer removal, *Acta Mater.*, Vol. 94, 2015B, pp. 71-80.

Hummelshøj, T.S.; Christiansen, T.L.; Somers, M.A.J.: Lattice expansion of carbon-stabilized expanded austenite, *Scripta Mater.*, Vol. 63, No. 7, 2010, pp.761-763.

Jespersen, F.N.; Hattel, J.H.; Somers, M.A.J.: Modelling the evolution of composition- and stress-depth profiles in austenitic stainless steels during low-temperature nitriding, *Mod. Simul. Mater. Sci. Eng.*, Vol. 24, No. 2, 2016, 025003 (31p).

Kücükyildiz, Ö.C.; Sonne, M.R.; Thorborg, J.; Hattel, J.H.; Somers, M.A.J.: Integrated Computational Modelling of Thermochemical Surface Engineering of Stainless Steel, *Proc. 24th IFHTSE Congres*, 2017, Nice.

Kücükyildiz, Ö.C.; Sonne, M.R.; Thorborg, J.; Somers, M.A.J.; Hattel, J.H.: 2018, in preparation.

Martinavičius, A.; Abrasonis, G.; Möller, W.: Influence of crystal orientation and ion bombardment on the nitrogen diffusivity in single-crystalline austenitic stainless steel, *J. Appl. Phys.*, Vol. 110, No. 7, 2011, 075907.

Moskalioviene, T.; Galdikas, A.: Stress induced and concentration dependent diffusion of nitrogen in plasma nitrided austenitic stainless steel, *Vacuum*, Vol. 86, No. 10, 2012, pp. 1552-1557.

Oddershede, J.; Christiansen, T.L.; Ståhl, K.; Somers, M.A.J.: Extended X-ray absorption fine structure investigation of nitrogen stabilized expanded austenite, *Scripta Mater.*, Vol. 62, No. 5, 2010, pp. 290-293.

Somers, M.A.J.; Christiansen, T.: Kinetics of microstructure evolution during gaseous thermochemical surface treatment, *J. Phase Equil. Diff.*, Vol. 26, No. 5, 2005, pp. 520-528.

Somers, M.A.J.; Christiansen, T.L.: Low temperature surface hardening of stainless steel. In: *ASM Handbook*, Volume 4D, Heat Treating of Irons and Steels, Eds. J. Dosset and G.A. Totten, 2014, pp. 439-450, ISBN: 978-1-62708-066-8.

Somers, M.A.J.; Christiansen, T.L.: Low temperature surface hardening of staibnless steels (Chapter 14) and Gaseous processes for low temperature surface hardening of stainless steel (Chapter 15). In: *Thermochemical Surface Engineering*, Eds. Mittemeijer, E.J. and Somers, M.A.J., WoodHead Publishing, 2015, pp. 557-614.

Somers, M.A.J.; Kücükyildiz, Ö.C.; Ormstrup, C.A.; Alimadadi, H.; Hattel, J.H.; Christiansen, T.L.; Winther, G.W.: "Residual stress in expanded austenite on stainless steel; origin, measurement and prediction", *Mater. Perform. Char.*, 2018, in print.

Templier, C.; Stinville, J.C.; Villechaise, P.; Renault, P.O.; Abrasonis, G.; Rivière, J.P.; Martinavičius, A.; Drouet, M.: On lattice plane rotation and crystallographic structure of the expanded austenite in plasma nitrided AISI 316L steel, *Surf. Coating Techn.*, Vol. 204, No. 16-17, 2010, pp. 2551- 2558.